



Hitting the material rail: An exploration of the comparison between Alloy Steel and AISI 1020

Rendy Satriawan^{1*} and Zhazira A.Baltabekova²

¹ Department of Mechanical Engineering, Faculty of Engineering, Universitas Negeri Padang, Padang, **INDONESIA**

² Institute of Metallurgy and Ore Beneficiation JSC, Satbayev University, Almaty, **KAZAKHSTAN**

*Corresponding Author: rendysatriawan660@gmail.com

DOI: <https://doi.org/10.58712/ie.v1i1.4>

Abstract: The rail track is a component that directly interfaces with the wheels. Generally, rail tracks serve as the foundation for trains, trams, and similar vehicles, bearing the friction and pressure from the wheels. Rail tracks have the potential for cracking and breaking due to various loads. Many studies have investigated the factors causing rail track fractures. This article employs the Finite Element Analysis (FEA) method using Solidworks research license software. In this simulation, two rail tracks with different materials, AISI 1020 and Alloy Steel, are numerically studied using Solidworks software to determine the most effective material for mitigating the risk of rail track fractures. The fracture risk is then calculated based on the material's fracture strength. The simulation results indicate that the fracture risk of rail tracks using Alloy Steel is lower than that of AISI 1020, thus recommending Alloy Steel as the more suitable material for rail tracks.

Keywords : Train; Railways; Finite element analysis; Material; Fracture risk

1. Introduction

A rail bar constitutes an indispensable component of railway infrastructure, functioning as a support base for the wheels of trains [1], [2]. Generally crafted from steel or other alloys renowned for their robustness, rail bars demonstrate exceptional durability against the various loads, pressures, and abrasions of train motion. Engineered to ensure stability and safety during train transit, they exhibit commendable resilience to temperature fluctuations and adverse weather conditions [3], [4]. Rail bars typically feature a unique profile characterized by a raised center and tapered edges, facilitating optimal support for train wheels [5].

Railway lines are typically categorized into two main sections: the substructure and the

Received: January 09, 2024. **Revised:** February 18, 2024. **Accepted:** March 06, 2024

© The Author(s) 2024. Published by Researcher and Lecturer Society. This is an Open Access article distributed under a [Creative Commons Attribution 4.0 International License](https://creativecommons.org/licenses/by/4.0/), which permits share and adapt in any medium, provided the original work is properly cited.

superstructure [6]. Commencing with the primary sections of the railway network that connect major cities or industrial centers, these main lines usually feature straighter tracks designed to accommodate heavy railway traffic, including freight and long-distance passenger trains [7]. Subsequently, branch lines are tracks that branch off the main lines, leading to less populated areas or specific destinations [8]. These branch lines are often shorter and may have lower maximum speeds than the main lines. Railway lines are commonly used to serve rural areas, small industries, or specialized installations such as ports or factory facilities [9].

The railway track bar is one of the critical elements in railway infrastructure that supports the weight of trains and their loads [10]. Nevertheless, like all metal structures, railway track bars are also susceptible to cracking and fracturing due to pressure, repetitive loads, and environmental factors. Analyzing the interaction between the wheel and the rail is crucial to understanding the railway system. Stress distribution becomes the main focus in evaluating how two materials interact when the wheel rotates on the rail. This highlights the importance of surface geometry, load conditions, and material properties in the context of the overall system. Researchers have investigated various aspects of this contact analysis, including the influence of geometry and contact behavior on critical stress distribution [11], [12]. Additionally, studies have explored damage effects such as surface cracks, plastic deformation, wear, and noise during operation [13]. In braking, previous research has often centered on thermal analysis between the wheel and brake pads, a crucial part of understanding the loads and system response.

In efforts to enhance the efficiency and reliability of sustainable transportation, research into suitable materials for vehicle structures becomes highly imperative. Comparing the strength of alloy steel with the adaptability of AISI 1020 can provide valuable insights for developing lighter yet robust and durable vehicles. By comprehending the characteristics of each material, engineers can devise vehicles with reduced weight without compromising strength and safety. This can improve fuel efficiency and diminish vehicles' carbon footprint, supporting a vision of more sustainable and environmentally friendly transportation [14]. This study aims to ascertain materials with load tolerance capabilities that can mitigate the risk of rail bar breakage. Comprehensive analysis is necessary to examine various interactions between the rail and wheel to pinpoint potential fracture points on the rail and explore optimal materials and designs to prevent it. The dynamic design of railway track components is influenced by numerous factors that must be considered in the design process [15], [16]. Consequently, this research will provide deeper insights into comparing alloy steel and AISI 1020 steel and their applications across various industries.

2. Methods

This study utilizes Solidworks software to design 3D models and assess stress and dimensional changes in railroad track designs [17]. Solidworks is a widely used

application for creating solid models, supporting professionals from various backgrounds, both novices and experts [18], [19]. In the process of geometric design simulation using Solidworks, the Finite Element Analysis (FEA) tool is employed, a feature provided by the software [20]. Stress-strain testing on railroad track structures adheres to specifications reviewed in various previous research projects.

The research procedure outlines a series of steps commencing with exploring and comprehending theories relevant to railroad models and systems, followed by examining materials and methodologies based on relevant literature. Subsequent steps involve the creation of rail and wheel models using the research version of Solidworks software. Within the framework of this study, we propose an innovative approach to design and develop sensor devices grounded in stress-strain analysis of railroad tracks [21], [22]. The final step entails an analysis of maximum stress on rails made of AISI 1020 and Alloy Steel as part of our research endeavor.

This analysis was conducted according to the UIC 60 Rail Profile standard, which has a 60 kg/m weight and is provided by the local railway operator. Details regarding the train wheel and rail were obtained from the local railway operator, including information on the wheel diameter of 965 mm (38 in), vertical load (maximum design load = 600 kN), and mechanical characteristics of the wheel (yield strength = 438 MPa; Young's modulus = 205 GPa; coefficient of friction = 0.3; material density = 7850 kg/m³; rotational velocity = 24.6 rad/s; ultimate tensile strength = 1080 MPa). The final stage of this research involves presenting the results and conclusions of the maximum stress analysis on the rail.

2.1 Rail bar

The rail bar was designed utilizing Solidworks software as a tool for drafting and conceptualizing it. The specifics and dimensions of this rail bar can be found in the illustration depicted in Figure 1.

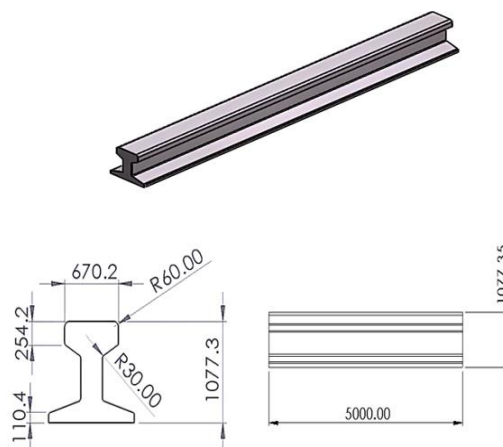


Figure 1: The three-dimensional specimen design of the rail track

2.2 Material

The analysis of the rail bar made of steel material is conducted based on the mechanical properties outlined in the following Table 1.

Table 1: Property of AISI 1020 and Alloy Steel

Property	AISI 1020	Alloy Steel
Elastic Modulus	200000 N/mm ²	210000 N/mm ²
Poisson's Ratio	0.29 N/A	0.28 N/A
Shear Modulus	77000 N/mm ²	79000 N/mm ²
Mass Density	7900 Kg/m ³	77000 Kg/m ³
Tensile Strength	420.507 N/mm ²	723.8256 N/mm ²
Yield Strength	351.571 N/mm ²	620.422 N/mm ²
Thermal Expansion Coefficient	1.5e-05/K	1.3e-05 /K
Thermal Conductivity	47 W/(m.k)	50 W/(m.k)
Specific Heat	420 j/(kg.k)	50 j/(kg.k)

3. Results and discussion

Upon completing the rail bar design, a simulation analysis was conducted on a 5-meter segment of the rail bar under a load of 600 kN. Two types of materials, AISI 1020 and Alloy Steel, were utilized. This analysis examines the von Mises stress, displacement, strain, and safety factors of Alloy Steel and AISI 1020 materials. The simulation results are depicted in the illustration presented in Figure 2.

3.1 Analisis von mises stress

From the simulation results aimed at determining the von Mises stress value, it is observed that the rail bar utilizing Alloy Steel (a) material exhibits a maximum stress value of 5,843,277.000 N/m² with a yield strength of 620,422,016.000 N/m², whereas for AISI 1020 (b), the maximum stress value recorded is 5,883,332.000 N/m² with a yield strength of 351,571,008.000 N/m². Consequently, Alloy Steel (a) demonstrates higher fracture resistance compared to AISI 1020 (b).

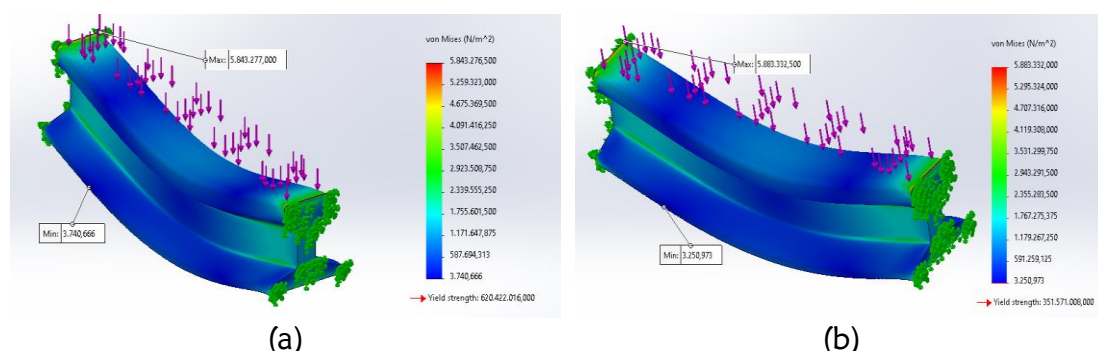


Figure 2: (a) Von mises stress Alloy Steel and (b) AISI 1020

3.2 Analysis displacement

The simulation results illustrated in Figure 3 It was found that the rail bar made of Alloy Steel (a) achieved a maximum displacement value of 0.02873986 mm, which is superior to AISI 1020 (b), recording a maximum displacement value of 0.03028318 mm. Thereby, the rail bar utilizing Alloy Steel (a) exhibits a slight improvement compared to AISI 1020 (b).

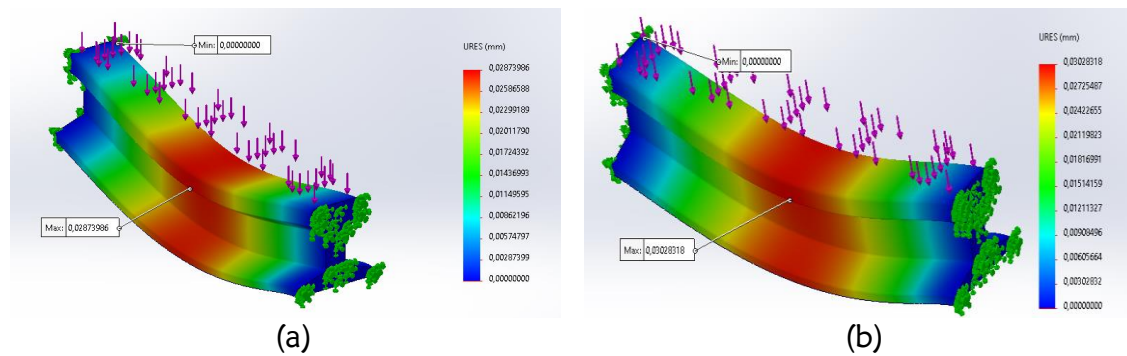


Figure 3: Displacement, (a) Alloy Steel and (b) AISI 1020

3.3 Analysis strain

The simulation results depicted in Figure 4 indicate that the rail bar employing Alloy Steel material (a) outperforms its counterpart utilizing AISI 1020 material (b). This is evident from the simulation, where Alloy Steel (a) exhibits a maximum strain value of 0.00002090, while AISI 1020 (b) registers a maximum strain value of 0.00002223.

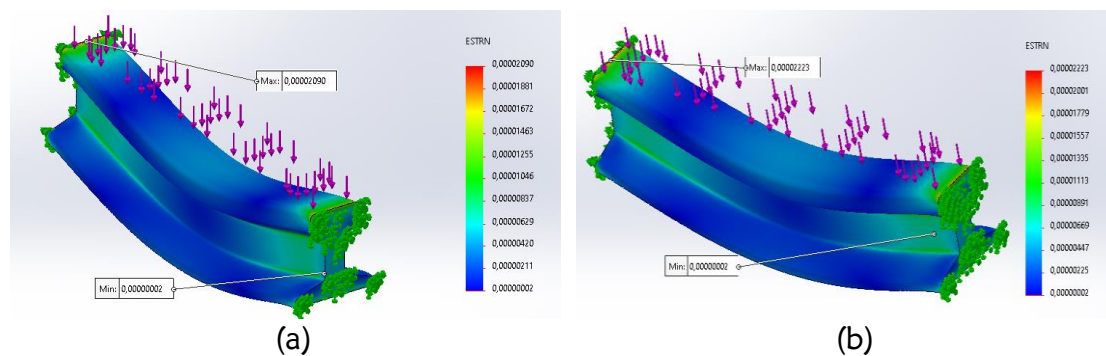


Figure 4: Strain, (a) Alloy Steel and (b) AISI 1020

3.4 Analysis factor of safety

The simulation results of the Factor of Safety (FOS) indicate that the rail bar made of Alloy Steel (a) achieves a minimum value of 106.177, significantly larger than AISI 1020 (b), which obtains a value of 59.757. Consequently, Alloy Steel (a) is preferable over AISI 1020 (b) for utilization.

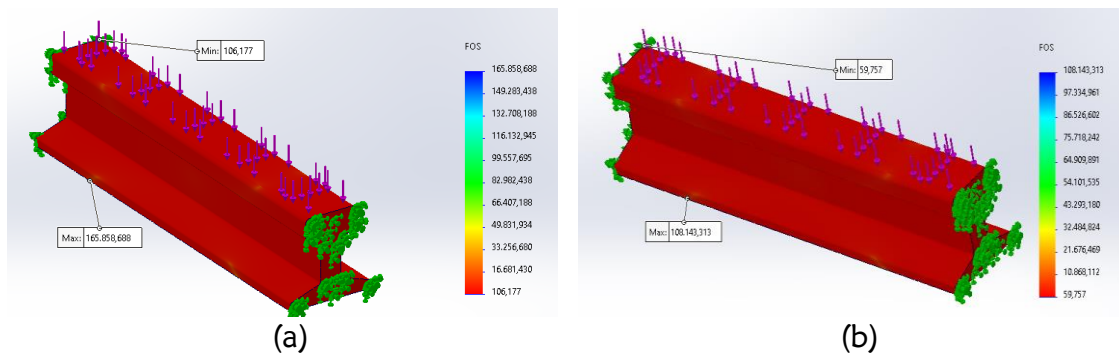


Figure 5: Factor of Safety, (a) Alloy Steel and (b) AISI 1020

4. Conclusion

Stress and strain analysis of railroad ties is crucial for understanding the wheel-rail interaction and predicting potential failures. This study compares alloy steel and AISI 1020 materials to assess their stress and strain tolerance. Using Solidworks, simulations were done on a 5-meter rail bar with a 600 kN load. Results showed lower stress, displacement, strain, and higher safety factors for Alloy Steel compared to AISI 1020. In conclusion, Alloy Steel rail bars outperform AISI 1020 in handling stresses and strains. Proper material selection is vital for rail infrastructure reliability and safety. Alloy Steel is recommended over AISI 1020 based on superior simulation performance, especially in load-bearing capacity, reducing fracture risk in rail bars.

Author contribution

Rendy Satriawan: Conceptualization, Investigation, Data Curation and Writing - Original Draft. Zhazira A.Baltabekova: Writing - Review & Editing, Formal analysis and Resources

Funding statement

This research received no specific grant from any funding agency in the public, commercial, or not-for-profit sectors.

Acknowledgements

The authors are grateful to the manufacturing laboratory for the use of computers for Solidworks simulations.

Conflict of interest statement

The authors declare no conflict of interest in this research and publication.

References

- [1] C. Du, S. Dutta, P. Kurup, T. Yu, and X. Wang, "A review of railway infrastructure monitoring using fiber optic sensors," *Sensors and Actuators, A: Physical*, vol. 303, p. 111728, 2020. <https://doi.org/10.1016/j.sna.2019.111728>
- [2] A. F. Esen, P. K. Woodward, O. Laghrouche, and D. P. Connolly, "Stress distribution in reinforced railway structures," *Transportation Geotechnics*, vol. 32, p. 100699, 2022. <https://doi.org/10.1016/j.trgeo.2021.100699>
- [3] S. Tetiranont, W. Sadakorn, N. T. Rugkhapan, and L. Prasittisopin, "Enhancing Sustainable Railway Station Design in Tropical Climates: Insights from Thailand's Architectural Theses and Case Studies," *Buildings*, vol. 14, no. 3, pp. 1–27, 2024. <https://doi.org/10.3390/buildings14030829>
- [4] C. Zhang, H. Kordestani, and M. Shadabfar, "A combined review of vibration control strategies for high-speed trains and railway infrastructures : Challenges and solutions," *Journal of Low Frequency Noise, Vibration and Active Control*, vol. 42, no. 1, pp. 272–291, 2023. <https://doi.org/10.1177/14613484221128682>
- [5] R. Patel, "The Permanent Way of the 1805 Congleton Railway: New Evidence from Fieldwork," *Industrial Archaeology Review*, vol. 42, no. 1, pp. 62–78, 2020. <https://doi.org/10.1080/03090728.2020.1716521>
- [6] L. Hausberger, T. Cordes, and F. Gschösser, "Life Cycle Assessment of High-Performance Railway Infrastructure, Analysis of Superstructures in Tunnels and on Open Tracks," *Sustainability (Switzerland)*, vol. 15, no. 9, pp. 1–18, 2023. <https://doi.org/10.3390/su15097064>
- [7] J. J. Pons, I. Villalba Sanchis, R. Insa Franco, and V. Yepes, "Life cycle assessment of a railway tracks substructures: Comparison of ballast and ballastless rail tracks," *Environmental Impact Assessment Review*, vol. 85, no. July, p. 106444, 2020. <https://doi.org/10.1016/j.eiar.2020.106444>
- [8] A. Sancho-reinoso *et al.*, "Mapping hierarchies of mobility in the Baikal Amur Mainline region : a quantitative account of needs and expectations relating to railroad usage," *Polar Geography*, vol. 45, no. 3, pp. 157–176, 2022. <https://doi.org/10.1080/1088937X.2022.2046195>
- [9] L. Santos y Ganges, "Historical Interrelationship of Railways and Cities from an Urban Viewpoint," *TST. Transportes, Servicios y Telecomunicaciones*, vol. 50, no. 50, pp. 16–41, 2023. <https://doi.org/10.24197/tst.50.2023.16-41>
- [10] A. Lovska, O. Fomin, V. Pišteš, and P. Kucera, "Dynamic Load Modelling within Combined Transport Trains during Transportation on a Railway Ferry," *Applied Sciences*, vol. 10, no. 16, pp. 1–15, 2020. <https://doi.org/10.3390/app10165710>
- [11] S. Gao, S. Chatterton, L. Naldi, and P. Pennacchi, "Ball bearing skidding and over-skidding in large-scale angular contact ball bearings : Nonlinear dynamic model with thermal effects and experimental results," *Mechanical Systems and Signal Processing*, vol. 147, p. 107120, 2021. <https://doi.org/10.1016/j.ymssp.2020.107120>
- [12] S. Zhang, D. Li, and Y. Liu, "Friction Behavior of Rough Surfaces on the Basis of

- Contact Mechanics: A Review and Prospects,” *Micromachines*, vol. 13, no. 11, pp. 1–23, 2022. <https://doi.org/10.3390/mi13111907>
- [13] Q. Lin, S. Jiang, H. Tian, H. Ding, W. Wang, and J. Guo, “Study on non-destructive testing of rail rolling contact fatigue crack based on magnetic barkhausen noise,” *Wear*, vol. 528–529, p. 204965, 2023. <https://doi.org/10.1016/j.wear.2023.204965>
- [14] K. J. Shah *et al.*, “Green transportation for sustainability: Review of current barriers, strategies, and innovative technologies,” *Journal of Cleaner Production*, vol. 326, p. 129392, 2021. <https://doi.org/10.1016/j.jclepro.2021.129392>
- [15] M. Gao *et al.*, “Dynamic modeling and experimental investigation of self-powered sensor nodes for freight rail transport,” *Applied Energy*, vol. 257, p. 113969, 2020. <https://doi.org/10.1016/j.apenergy.2019.113969>
- [16] G. Lazorenko, A. Kasprzhitskii, and T. Nazdracheva, “Anti-corrosion coatings for protection of steel railway structures exposed to atmospheric environments: A review,” *Construction and Building Materials*, vol. 288, p. 123115, 2021. <https://doi.org/10.1016/j.conbuildmat.2021.123115>
- [17] M. Arif, H. Rosmi, M. K. Omran, M. Noor, and F. Mohd, “Stanchion Re-design for Kuala Lumpur Additional Vehicle (KLAV) 27 Project based on SolidWorks Simulation,” *Progress in Engineering Application and Technology*, vol. 4, no. 2, pp. 1129–1139, 2023. <https://doi.org/10.30880/peat.2023.04.02.116>
- [18] B. R. Hunde and A. D. Woldeyohannes, “Future prospects of computer-aided design (CAD) – A review from the perspective of artificial intelligence (AI), extended reality, and 3D printing,” *Results in Engineering*, vol. 14, no. April, p. 100478, 2022. <https://doi.org/10.1016/j.rineng.2022.100478>
- [19] Waskito, A. Fortuna, F. Prasetya, R. E. Wulansari, R. A. Nabawi, and A. Luthfi, “Integration of Mobile Augmented Reality Applications for Engineering Mechanics Learning with Interacting 3D Objects in Engineering Education,” *International Journal of Information and Education Technology*, vol. 14, no. 3, pp. 354–361, 2024. <https://doi.org/10.18178/ijiet.2024.14.3.2057>
- [20] G. Kumar, R. Singh, P. Kumar, T. Rajput, E. Neha, and Y. Shrivastava, “Design and Analysis of an Automatic Seed Sowing Machine Using SolidWorks and ANSYS Tools,” in *Advances in Engineering Design*, 2020, pp. 595–602. https://doi.org/10.1007/978-981-33-4684-0_60
- [21] C. Ballester, V. Muñoz, D. Copaci, L. Moreno, and D. Blanco, “Sensors and Actuators: A . Physical Design of a soft sensor based on silver-coated polyamide threads and stress-strain modeling via Gaussian processes,” *Sensors and Actuators: A. Physical*, vol. 367, p. 115058, 2024. <https://doi.org/10.1016/j.sna.2024.115058>
- [22] P. Sharan, S. Mishra, and A. M. Upadhyaya, “Optical Fiber Technology The development of laboratory downscale rail-wheel test rig model with optical sensors,” *Optical Fiber Technology*, vol. 77, p. 103287, 2023. <https://doi.org/10.1016/j.yofte.2023.103287>